NAVAL POSTGRADUATE SCHOOL
Monterey, California

THESIS

MULTISPECTRAL ANALYSIS OF NIGHTTIME LOW CLOUDS OVER THE OCEAN

by

James D. Dykes

March 1991

Thesis Advisor Carlyle H. Wash

Unclassified

security classification of this page

REPORT DOCUMENTATION PAGE

1a Report Security Classification Unclassified			1b Restrictive Markings
2a Security Classification Authority			3 Distribution/Availability of Report
2b Declassification/Downgrading Schedule			Approved for public release; distribution is unlimited.
4 Performing Organization Report Number(s)			5 Monitoring Organization Report Number(s)
6a Name of Performing Organization Naval Postgraduate School	6b Office Symbol *(if applicable)* 35		7a Name of Monitoring Organization Naval Postgraduate School
6c Address *(city, state, and ZIP code)* Monterey, CA 93943-5000			7b Address *(city, state, and ZIP code)* Monterey, CA 93943-5000
8a Name of Funding,Sponsoring Organization	8b Office Symbol *(if applicable)*		9 Procurement Instrument Identification Number
8c Address *(city, state, and ZIP code)*			10 Source of Funding Numbers
			Program Element No / Project No / Task No / Work Unit Accession No

11 Title *(include security classification)* MULTISPECTRAL ANALYSIS OF NIGHTTIME LOW CLOUDS OVER THE OCEAN

12 Personal Author(s) James D. Dykes

13a Type of Report	13b Time Covered	14 Date of Report *(year, month, day)*	15 Page Count
Master's Thesis	From To	March 1991	51

16 Supplementary Notation The views expressed in this thesis are those of the author and do not reflect the official policy or position of the Department of Defense or the U.S. Government.

17 Cosati Codes			18 Subject Terms *(continue on reverse if necessary and identify by block number)*
Field	Group	Subgroup	Low cloud analysis, radiative transfer, fog, satellite imagery,

19 Abstract *(continue on reverse if necessary and identify by block number)*

Multispectral imagery is used for the analysis of nighttime low clouds whose cloud top temperatures are similar to that of the ocean surface. At night AVHRR channel 3 (3.7 μm) and channel 4 (10.8 μm) brightness temperature differences distinguish the presence of low stratus and fog from the ocean surface improving upon the channel 4 analysis alone. However, the effect of moisture attenuation in channel 4 offsets this temperature difference and impact thresholds which determine low cloud extent. Radiative transfer simulations using different moisture profiles helped to determine threshold adjustment. This thesis uses one of two sets of thresholds depending on moisture extent in an enhancement scheme to discriminate clear areas, and scattered, broken and overcast clouds on different summertime imagery cases over the ocean. Two cases are illustrated thoroughly and the technique was also applied to eight other cases. Results agreed for the most part with surface observations and visible GOES from the previous day. The multi-channel technique improved most or all deficiencies of the single channel analysis in all the cases except one where only some deficiencies were improved. The color enhancement provides a clear, qualitative picture of nighttime low cloud.

20 Distribution/Availability of Abstract	21 Abstract Security Classification	
☒ unclassified/unlimited ☐ same as report ☐ DTIC users	Unclassified	
22a Name of Responsible Individual Carlyle H. Wash	22b Telephone *(include Area code)* (408) 646-2295	22c Office Symbol MR(Wx)

DD FORM 1473,84 MAR

83 APR edition may be used until exhausted
All other editions are obsolete

security classification of this pag

Unclassific

Approved for public release; distribution is unlimited.

Multispectral Analysis of Nighttime Low Clouds over the Ocean

by

James D. Dykes
Captain, United States Air Force
B.A., California State University, Sacramento, 1985

Submitted in partial fulfillment of the
requirements for the degree of

MASTER OF SCIENCE IN METEOROLOGY

from the

NAVAL POSTGRADUATE SCHOOL
March 1991

ABSTRACT

Multispectral imagery is used for the analysis of nighttime low clouds whose cloud top temperatures are similar to that of the ocean surface. At night AVHRR channel 3 (3.7 μm) and channel 4 (10.8 μm) brightness temperature differences distinguish the presence of low stratus and fog from the ocean surface improving upon the channel 4 analysis alone. However, the effect of moisture attenuation in channel 4 offsets this temperature difference and impact thresholds which determine low cloud extent. Radiative transfer simulations using different moisture profiles helped to determine threshold adjustment. This thesis uses one of two sets of thresholds depending on moisture extent in an enhancement scheme to discriminate clear areas, and scattered, broken and overcast clouds on different summertime imagery cases over the ocean. Two cases are illustrated thoroughly and the technique was also applied to eight other cases. Results agreed for the most part with surface observations and visible GOES from the previous day. The multi-channel technique improved most or all deficiencies of the single channel analysis in all the cases except one where only some deficiencies were improved. The color enhancement provides a clear, qualitative picture of nighttime low cloud.

LIST OF FIGURES

ACKNOWLEDGEMENTS

Everyone in the Meteorology Department and support system have been a great help to me. My deepest gratitude goes to Dr. Carlyle Wash, my thesis advisor, who through his professional guidance better abled me to present the best possible product. Special thanks goes to Dr. Philip Durkee's whose expertise helped me along the way and to Dr. Kenneth Davidson for his helpful advice and corrections. Thanks to Capt Tom Neu, former NPS student, for taking valuable time out to introduce me to the Idea Lab. I owe Mr. Craig Motell a great deal for his expertise and long work hours on my account. Thanks to Mr. Thomas Lee for his personal contributions and data support. This thesis is dedicated to my loving future wife, Carolyn, who came over from her home in Canada to give me support during the final days before graduation.

I. INTRODUCTION

Past experiences in the use of satellite-sensed imagery have shown that there are severe operational limitations in distinguishing and forecasting nighttime low clouds due to poor spatial and radiometric resolution of the imagery and limited enhancement display capability. At night, low clouds are not detected due to low thermal contrast between surface temperatures and cloud temperatures. Also, low cloud formations may cover areas smaller than the field of view (FOV), thereby appearing in the imagery warmer or cooler than they really are. This thesis will address the problem of detecting these clouds.

This problem of fog detection is particularly relevant during the summer over the North Atlantic and North Pacific Oceans, and Bering Sea (as well as in the southern oceans). At low levels, the ocean dominates the cloud and weather patterns. In the summer, the advection of warm moist air from the south over cold water results in widespread fog and low clouds, whose temperatures are near that of the sea surface.

These conditions have significant impact on military operations in the region and require greater attention by the forecaster. For example, weather conditions required for the launch and recovery of aircraft are a big concern at Shemya AFB, a small remote island on the Aleutian Chain. Aircraft are particularly sensitive to cloud ceiling heights, visibilities and crosswinds, especially at Shemya, where all these parameters are usually near critical values for safe aviation operations.

Surface and upper-air data is sparse in the region, so that the forecaster must rely on satellite imagery. At Shemya, Automatic Picture Transmission (APT) is available as a direct readout from the Advanced Very High Resolution Radiometer (AVHRR) on the NOAA (National Oceanic and Atmospheric Administration) polar orbiting satellites. Imagery is received about eight times a day with visible and infrared (IR) during the day and IR only at night. Fig. 1 is an example of this product. But, this source of data has its limitations as well.

Visible imagery is not available early in the morning or at night. With IR only, it is difficult to distinguish low clouds from the surface as well as distinguishing between cloud boundaries and sea surface temperature boundaries. During the summertime, a strong inversion is common resulting in cloud tops warmer than the ocean surface below. On satellite imagery with standard enhancement, these clouds, labeled "black stratus" by the operational forecaster, may appear unexpectedly darker than the ocean.

Recent research (d'Entremont 1986; d'Entremont and Thomason 1987; Crosiar et al. 1989; Dozier 1981; Eyre et al. 1984; Ellrod et al. 1989; Olesen and Grassl 1985; Saunders and Kriebel 1988) has shown that intercomparisons between near-IR and thermal IR frequencies reveal the presence of low clouds. In particular, digital imagery from the NOAA AVHRR channels 3 (3.7 μm), 4 (11.5 μm), and 5 (12.5 μm) can be utilized for this purpose. The key is the difference in brightness temperatures between channel 3 and the others. But, limitations are inherent in the technique. Particularly, atmospheric effects, i. e. attenuation due to moisture, aerosols, etc., need to be quantified to help make adjustments in the technique. The goals in this thesis are to improve upon the conventional analysis of low clouds by applying this multispectral method to scenes of low clouds over oceans at night. A threshold of the brightness difference will be used to determine the presence of cloud and adjustments will be made to the thresholds to correct for moisture effects.

Recent developments concerning bispectral techniques and radiative processes of clouds are discussed in Chapter II. Chapter III presents results of moisture effects using the LOWTRAN7 radiative transfer model. This provides a quantitative perspective of radiative transfer and the moisture effect on brightness differences for the methodology introduced in Chapter IV. Here, data sources and the implementation of the technique are described. Chapter V presents results of the technique on several cases beginning in depth with two scenes, one from the Pacific and one from the Atlantic. Chapter VI presents conclusion and recommendations.

Fig. 1. Example of satellite imagery via APT routinely analyzed at Shemya. The left half is the infrared channel and the right half the accompanying visual channel. This pass covered the Kamchatka Peninsula and the western most islands of the Aleutian Chain.

II. BACKGROUND

The success in multispectral analysis of low clouds depends on the different processes which affect radiative transfer within each infrared channel measured by the AVHRR. Channel 3 plays a primary role, because at this wavelength emissivities of low liquid water clouds are significantly less than unity while in channels 4 and 5 the emissivities are nearly one (Hunt 1973). Table 1 shows tabulated values for cloud radiative properties from Hunt (1973) as arranged by d'Entremont (1986). Therefore, in a low cloud situation, the channel 3 brightness temperature, T_3 , will be cooler than T_4 or T_5 by as much as 5 K due to the lower channel 3 emissivity, i. e. $T_3 - T_5$ or $T_3 - T_4$ will be negative.

On the other hand, channel 3 emissivities approach unity for land and ocean surfaces. Channels 4 and 5 emit from these surfaces close to a blackbody as well. As a result, brightness temperatures from satellite measured radiances emitted from cloudfree regions will be close to the same in all three channels.

The relationships between emissivity, reflectivity, transmissivity, droplet mode radius and optical depth are illustrated in Table 1) from Hunt (1973) as compiled by d'Entremont (1986). Lower emissivity for a given wavelength implies that the reflectivity and/or transmissivity are nonzero. This stems from the relation that the sum of transmissivity, emissivity, and reflectivity is one. If a cloud layer through which direct radiation must propagate is optically thin, then the direct transmissivity is nonzero and there is a contribution of total upwelling radiation from below the cloud. On the other hand, if the layer is optically thick (optical depth > 50), transmissivity is zero and emissivity is less than 1 due to nonzero reflectivity. These properties will vary according to the droplet mode radius; smaller droplets have lower emissivities, particularly in channel 3. The resulting upwelling radiation from low clouds results in brightness temperatures lower in channel 3 than in the other longer infrared channels provided the actual surface temperatures are not too warm.

Table 1. **CLOUD RADIATIVE PROPERTIES.** (from Hunt 1973 as arranged by d'Entremont 1986).

		Emissivity			Reflectivity			Transmissivity		
Droplet mode radius	Total cloud optical depth	Ch 3	Ch 4	Ch 5	Ch 3	Ch 4	Ch 5	Ch 3	Ch 4	Ch 5
10 μm	10	0.80	0.99	0.99	0.10	0	0	0.10	0.01	0.01
10 μm	> 50	0.90	1.00	1.00	0.10	0	0	0	0	0
4 μm	5	0.35	0.97	0.97	0.21	0	0	0.44	0.03	0.03
4 μm	10	0.58	0.99	0.99	0.25	0	0	0.17	0.01	0.01
4 μm	> 50	0.74	1.00	1.00	0.26	0	0	0	0	0

If the surface is warm enough and the cloud layer is optically thin, the upwelling radiance from the surface that gets transmitted through the cloud can contribute enough to the total radiance to offset the lower emissivity effect of channel 3, i. e. T_3 from the cloud plus the ground will exceed T_4 or T_5. Much of the time, however, fog and low clouds have optical depths sufficient to limit the upwelling contribution particularly over the oceans. But, when this is not the case, these clouds would be cool enough compared to the surface to easily be detected with channel 4 or 5 alone. In choosing a threshold of brightness difference in determining cloudiness, the optically thin case would have to be eliminated as not cloudy.

Although there is very little atmospheric water vapor attenuation in channel 3, water vapor significantly attenuates radiances in channels 4 and 5 resulting in cooler brightness temperatures, thus affecting the resulting brightness differences. Channel 5 is used in the following discussion since it is affected by moisture the most. In a clear air path the difference, $T_3 - T_5$, will be close to zero when no water vapor is present. But with water vapor, $T_3 - T_5$, will be positive. With the addition of clouds, $T_3 - T_5$ would normally be negative if the moisture effect on channel 5 were low. However, if the path from the cloud top is moist enough, $T_3 - T_5$ will be positive once again. For a given region of locally uniform moisture content, $T_3 - T_5$ would always be less over clouds than over clear areas. In ad-

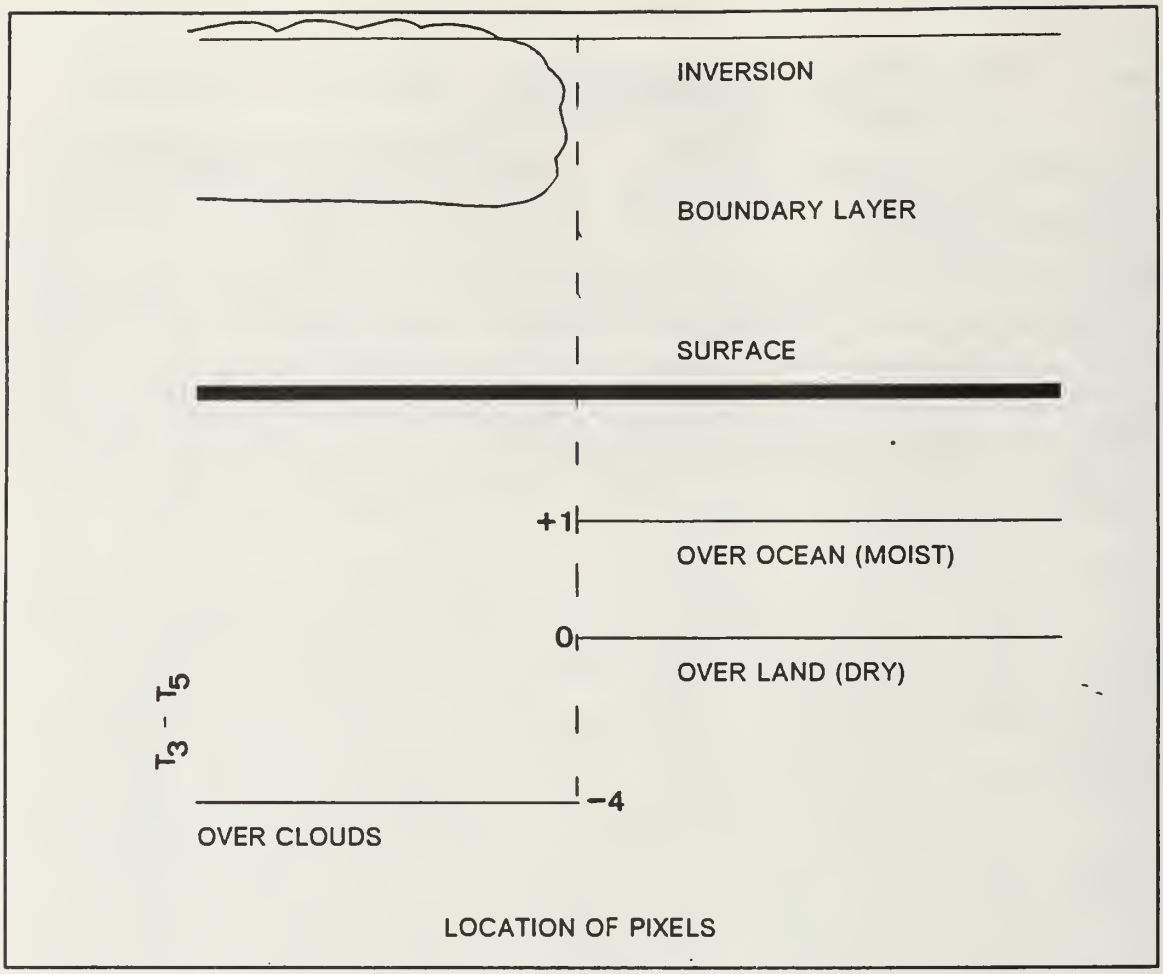

Fig. 2. The contrast between brightness differences. Examples of resulting dry and moist differences over a clear region are compared to that of a cloudy region.

dition, much of the moisture resides below existing cloud tops. The diagram in Fig. 2 illustrates the contrast between $T_3 - T_5$ for over clouds and that over a clear surface. T_5 from the ocean over which moisture resides will be cooler than from land. Thus, as will be seen quantitatively in the next chapter, $T_3 - T_5$ would generally be even more negative for a moist boundary layer resulting in better contrast (Lee, personal communication 1990).

A variable affecting moisture amount in the boundary layer is sea surface temperature. From Lee (personal communication 1990) and Crosiar et al. (1989), colder regions lying towards the north contain less atmospheric moisture than

warmer more southerly regions, simply because the sea surface temperature controls the air temperature in the boundary layer thereby controlling the ability for the air to hold moisture. Resulting brightness differences are significantly more positive in clear FOVs over the cooler northern ocean surface waters.

Discrepancies in image interpretations result from certain satellite sensor limitations. Allam (1986) demonstrated using multispectral techniques for NOAA-7 the existence of a misregistration of about one-quarter of a pixel between channels 3 and 4. This results in edging in the differenced image. This effect may be seen in one of the cases in this thesis, but this discrepancy does not seem to adversely affect the technique.

A possibly more serious effect of the limited sensor is the noise that is produced, particularly in channel 3 in the colder regions. Channel 3 noise has been a recurring problem with the AVHRR instrument. Dozier (1981) derived a radiance-temperature relationship by integrating the product of the Planck function and the response function of a NOAA6 sensor. Fig. 3 presents the radiances calculated by Dozier for channels 3 and 4 from 100 to 1000 K. Channel 3 changes more quickly in the colder temperatures and radiances are much lower for a given temperature under 300 K than in channel 4. There the Planck function is more sensitive to variations in temperature and noise in channel 3 than in channel 4. Thus, channel 3 noise becomes more amplified when sensing colder regimes.

Cloud coverages of partially filled FOVs were determined by using the differences in nonlinearity of the Planck function for each of the different wavelengths. Dozier's graph in Fig. 3 shows how the nonlinearity of the radiance-temperature relation plays a role. Consider a mixed scene composed of cloud at temperature T_{cld} occupying a portion ρ of a FOV and the clear area of temperature T_{sfc} taking the rest of the $1 - \rho$ portion of the FOV. The upwelling radiance will be a linear combination of the cloud and surface radiances given by

$$L_{j,sat} = (1 - \rho)L_{j,clr} + \rho L_{j,cld} \qquad (1)$$

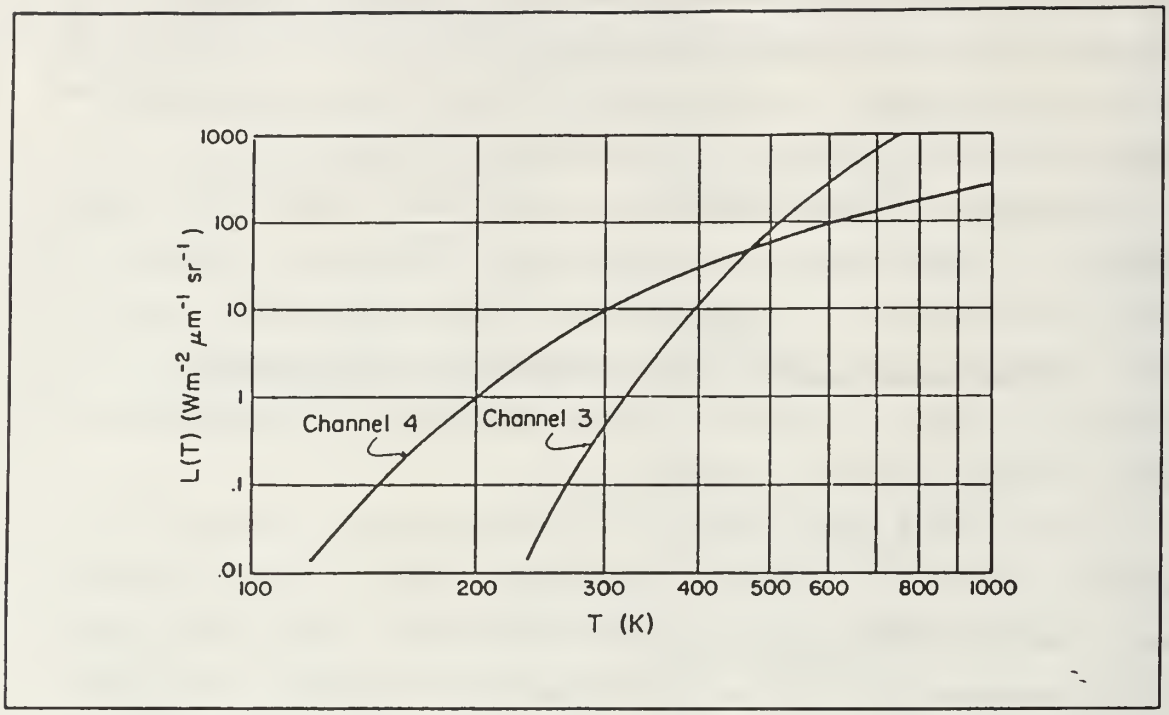

Fig. 3. NOOA6 radiances for channels 3 and 4 vs. temperature. (As calculated by Dozier 1981).

where $L_{j,clr}$ and $L_{j,cld}$ are radiances from cloudfree and cloudfilled scenes, respectively, at channel j. $L_{j,sat}$ can be measured and converted to a brightness temperature using the inverted Planck function. Since the shift in the peak in the Planck function is toward shorter wavelengths as temperature increases, the radiant contribution to channel 3 increases more rapidly at higher temperatures, than in channel 4. For a partially filled FOV, the comparisons between the surface and cloud contributions are different in each AVHRR channel. The warmer portion of a FOV in channel 3 would contribute more to the total radiance than would the warmer portion of channels 4 and 5. Therefore, one can determine cloud temperatures of partially filled FOVs using the brightness temperature of a completely clear surface (or even without it) and by using the channel 3 and 4 brightness temperatures.

D'Entremont (1986) used both of the above concepts to analyze cloud height and coverage for low- and midlevel clouds. For each channel of the AVHRR,

he calculated radiances based on a comprehensive radiative transfer model using radiative properties from Hunt (1973). Each radiance calculation can be paired with any combination of radiances resulting from partially filled FOVs giving distinct pairs of values for cloud top temperature (corresponding to height) and cloud coverage. A few samples illustrating this technique demonstrated the soundness of the principle. Still, it is unrealistic to expect this technique to perform well in general. Small uncertainties in surface emissivities, surface temperatures, cloud radiative properties and atmospheric profiles greatly affect the final results. Because surface temperature plays a major role in the technique, one can expect a dominant effect in the analysis even with partially filled FOVs. Some of these limitations will be reduced when specifying a specific ocean region for analysis and using a threshold for determining the presence of low clouds rather than attempting to determine the amount of cloudiness in a given FOV.

A British team at Bracknell University developed an analysis scheme for detecting low clouds displaying images in color (Eyre et. al. 1984). Brightness temperatures from AVHRR channel 4 and brightness differences, ΔT between channels 3 and 4 were digitized such that for $\Delta T < 0.5K$, a range of colors is used depending on brightness temperatures in channel 4; for $\Delta T > 2.5K$, a range of grey shades is used depending on temperature in channel 4; and for intermediate values of ΔT, a combination of the above is used. This approach picks out areas of low clouds which only partially cover a pixel. Features are easily interpreted from a "natural" color display, thus giving a qualitative analysis of low clouds. The same limitations that restricted d'Entremont's technique affect this one as well. However, results revealed cloudy areas over Great Britain which otherwise would not be detected by surface observations.

The multispectral technique has been used with GOES data from two sounding channels, bands 8 and 12, with similar success (Ellrod et al. 1989). Although resolutions are low (8 km for band 8 and 16 km for band 12), the advantage is that images can be obtained hourly at the same place. Fig. 4 plots both bands over a line drawn through an area of overcast stratus. Band 12 (3.9 μm) with its sharper gradients delineates temperatures better than band 8 (11.2

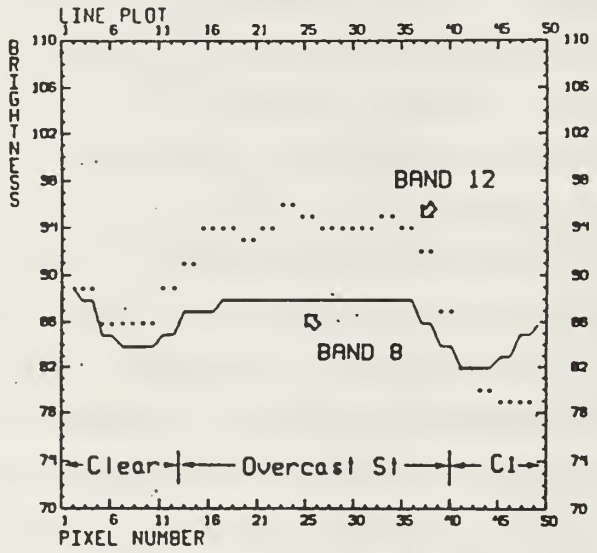

Fig. 4. Plots of digital brightness for GOES-VAS bands 8 and 12. (from Ellrod et al. 1989).

μm), but their differences show edges even more distinctly. The greater difference between the bands occurs over the area of stratus while over the clear area the difference is near zero.

As the various concepts discussed above are reviewed in the determination of the presence of low clouds over the ocean, it is concluded that the effect of atmospheric water vapor on the transfer of radiation is the primary concern. In the next chapter, we will quantify to a first order the affect of moisture in the atmosphere on radiative transfer in each channel of the AVHRR and on the brightness differences.

III. RADIATIVE TRANSFER AND MOISTURE EFFECTS

To quantify the atmospheric effects on the satellite measured brightness temperatures, a radiative transfer model, LOWTRAN7, was used. Developed by Air Force Geophysical Laboratories, LOWTRAN7 (AFGL 1989) models all the important constituents and aerosols in the atmosphere that photons would encounter in their paths from a background to a satellite sensor. It calculates atmospheric transmittance and all the various contributions to radiance for all the infrared wavelengths. The program includes representative temperature and moisture profiles from which a midlatitude summer atmospheric profile was chosen. From there, modifications in the moisture were made to show the magnitude of variation in the resulting AVHRR channel brightness temperature. In addition, boundaries at 1 and 2 km in altitude were created to represent tops of optically thick clouds with emissivity less than unity for channel 3. Wavelength regimes studied include frequency ranges from 3.552 μm to 3.929 μm to represent AVHRR channel 3, 10.256 μm to 11.364 μm for channel 4 and 11.494 μm to 12.500 μm for channel 5. The total transmittance and radiance from the surface or cloud top to 100 km in the zenith were evaluated for every 5 cm^{-1}. The integrated radiance and average transmittance throughout each frequency range were calculated assuming a perfect response function. From the radiances at each channel, brightness temperatures were evaluated using the inverse Planck function. These theoretical temperatures were compared between channels to determine the differences due to different moisture conditions.

The model's midlatitude summer profile at 45 °N in July was chosen to represent the standard temperature, pressure and moisture profile appropriate for objectives of this research. The surface temperature was set at 294 K. Also, included in the experiments were a completely dry and completely saturated profile. In addition, a more realistic profile to account for ocean effects included a boundary layer 1 km thick with a dry atmosphere above.

For sensing over the ocean, aerosols introduced into the atmosphere from the ocean surface were accounted for by LOWTRAN7's Navy Maritime model (AFGL 1989). The resulting radiances in all channels were slightly lower due to increased attenuation. Though not a major factor, the aerosol contribution effect was included from here on for completeness.

Using the model's standard midlatitude summer profile with no clouds, the brightness temperatures in channels 3 and 4 were about 3 K lower than the surface temperature (294.2 K) whereas in channel 5 the difference averaged 4 K (see STANDARD column of Table 2). As expected, the average atmospheric transmittance was significantly lower in channel 5 as well. Due to moisture attenuation in channel 5, $T_3 - T_5$ was positive by about 1.5 K. The radiative computations on the same temperature profile but with absolutely no moisture (see DRY column of Table 2) resulted in higher transmittance. Both T_4 and T_5 nearly equaled the actual temperature of the surface, while T_3 was slightly less Thus, moisture was affecting radiative transfer in channel 5 more than the others. Any brightness differences between channels were less than a half degree for this case.

For the other moisture extreme, the atmosphere was made completely saturated throughout layers extending to 25 km. This provided the theoretically largest difference between channels 3 and 4 or 5 due to moisture effects for a given sounding.

Table 2. BRIGHTNESS TEMPERATURES FOR A CLOUDLESS ATMOSPHERE USING LOWTRAN7. The radiative path was through the model's standard midlatitude atmosphere and started at the surface at 294.2 K.

		STANDARD		DRY		MOIST		BNDRY LYR MOIST	
j	ε_j	t_j	T_j (K)	t_j	T_j (K)	t_j	T_j (K)	t_j	T_j (K)
5	1.00	0.57	290.1	0.96	293.6	0.29	285.9	0.30	289.8
4	1.00	0.70	291.6	0.96	293.6	0.45	288.6	0.43	290.7
3	1.00	0.75	291.5	0.89	293.2	0.50	289.7	0.78	291.4
$T_3 - T_5$			+1.4		−0.4		+3.6		+1.6
$T_3 - T_4$			−0.1		−0.4		+1.1		+0.7

From the midlatitude summer profile, channel 5 transmittance decreased the most dropping to .29. The T_5 brightness temperature was 285.9 K, 8.3 K cooler than the actual surface temperature. Channel 4 was affected somewhat less ($t = .45$), and channel 3 still lesser yet ($t = .50$). This gave a difference between T_3 and T_5 of as much as positive 3.6 K (see MOIST column of Table 2).

In a more realistic oceanic scenario, a boundary layer was assumed to be 1 km thick in which moisture content is primarily influenced by the ocean surface. The air mass above 1 km may be dry due to subsidence and a capping inversion with a possible low cloud deck below. A profile to include moisture to saturation in the lowest 1 km and dry above was also included in Table 2 (see BNDRY LYR MOIST column). T_5 and T_4 decreased 4.4 K and 3.5 K, respectively, from the actual surface temperature compared to 8.3 K and 5.6 K for the moist case, which shows that a large proportion of the attenuation due to moisture occurred within the boundary layer. The resulting brightness differences between the channels were still positive but less. $T_3 - T_5$ became 1.6 K while $T_3 - T_4$ became 0.7 K.

The simulated brightness temperatures for channels 3, 4 and 5 from a 1-km cloud top in the standard, dry and moist atmospheres are presented in Table 3. Naturally, the BNDRY LYR MOIST profile was not included since this layer would lie below the cloud tops. The differences between channels 3 and 4 or 5 calculated from Table 3 for varying cloud emissivities is presented in Table 4.

Table 3. BRIGHTNESS TEMPERATURES FOR A 1-KM CLOUD TOP. Temperature of the cloud top was 289.7 K.

		STANDARD		DRY		MOIST	
j	ε_j	t_j	T_j (K)	t_j	T_j (K)	t_j	T_j (K)
5	1.00	0.74	287.2	0.97	289.1	0.48	284.1
4	1.00	0.83	288.0	0.97	289.2	0.62	285.9
3	0.90	0.80	285.6	0.94	286.5	0.74	284.9
3	0.85	0.80	284.7	0.94	285.3	0.74	283.9
3	0.80	0.80	283.7	0.94	284.1	0.74	282.9
3	0.75	0.80	282.5	0.94	282.7	0.74	281.8

Table 4. **BRIGHTNESS DIFFERENCES FOR A 1-KM CLOUD TOP.** Differences were calculated with the results from Table 3.

	STANDARD		DRY		MOIST	
ε_3	$T_3 - T_5$	$T_3 - T_4$	$T_3 - T_5$	$T_3 - T_4$	$T_3 - T_5$	$T_3 - T_4$
0.90	−1.6	−2.4	−2.6	−2.7	+0.8	−1.0
0.85	−2.5	−3.3	−3.7	−3.9	−0.2	−2.0
0.80	−3.5	−4.3	−5.0	−5.1	−1.2	−3.0

Emissivities were less than unity for channel 3, but were assumed to remain as unity for channels 4 and 5. A range of cloud emissivities for channel 3 was run in order to include clouds of different droplet mode radii, lower emissivities resulting from smaller droplets (Hunt 1972). Results in Table 4 show that as emissivity is decreased, brightness differences between channels 3 and 4 or 5 became more and more negative. Thus, clouds with smaller droplets, such as thick fog, would be more easily identified. Also, note that $T_3 - T_4$ was invariably more negative than $T_3 - T_5$ whether the path was standard, moist, or dry, although, from the DRY column on Table 4, the difference was small. The differences, $T_3 - T_4$ range from -2.4 K to -4.3 K for the standard atmosphere, -2.7 K to -5.1 K for the dry case and -1.0 K to -3.0 K for the moist case. The results show that liquid water clouds will lower T_3 versus T_4 or T_5. This also implies that brightness differences using channel 4 are more suitable than with channel 5 for low cloud analysis.

Given that atmospheric moisture lies below 1 km, a comparison was made between brightness differences for the clear profile with moisture below 1 km and the profile with the dry atmosphere over the 1-km cloud top. Compare the brightness differences in the BNDRY LYR MOIST column of Table 2 to that in the DRY column of Table 4. For a channel 3 cloud emissivity of .85, the range between brightness differences was 5.5 K using T_4 in the difference. Lower cloud emissivities in channel 3 implied even greater contrast in the $T_3 - T_4$ between the cloudy and clear pixels. Therefore, more atmospheric moisture within the boundary layer results in higher contrast between cloudfree and cloudy areas

assuming that we are comparing FOVs within similar air masses. This is consistent with results from Lee (personal communication 1990), discussed in the previous chapter.

The brightness temperatures for channels 3, 4 and 5 from a 2-km cloud top are presented in Table 4 similarly to Table 3. Again, the differences between channels 3 and 4 or 5 using results from Table 3 for varying cloud emissivities are presented in Table 4. These results show that moisture plays a lesser role in attenuation of radiation. Since transmittance was higher for all cases with 2-km cloud tops, simulated temperatures of the cloud tops were closer to the resulting brightness temperatures than in the 1-km case. With less moisture attenuation, brightness differences, $T_3 - T_5$ and $T_3 - T_4$, from 2-km cloud tops were more negative than from 1-km cloud tops. For example, the range of $T_3 - T_4$ for the standard profile is -3.1 K to -5.3 K for the 2-km cloud top case versus -2.4 K to -4.3 K for the 1-km case. Higher stratus clouds (2-km tops) will be more easily analyzed than lower clouds (1-km tops) of the same properties since less moisture attenuation in the path allows for greater differences between channels 3 and 4.

The LOWTRAN7 results show the range of brightness temperature differences for varying amounts of atmospheric water vapor in the path of the radiation being observed. The presence of high moisture in the path reduced the brightness differences over clouds to approximately -1 K for $T_3 - T_4$ and even weakly positive for $T_3 - T_5$. In addition, brightness differences over clear areas

Table 5. BRIGHTNESS TEMPERATURES FOR A 2-KM CLOUD TOP. Temperature of the cloud top was 285.2 K.

		STANDARD		DRY		MOIST	
j	ε_j	t_j	T_j (K)	t_j	T_j (K)	t_j	T_j (K)
5	1.00	0.86	283.5	0.98	284.7	0.65	281.2
4	1.00	0.91	284.1	0.98	284.8	0.76	282.7
3	0.90	0.86	281.1	0.95	282.2	0.80	281.0
3	0.85	0.86	280.0	0.95	281.1	0.80	280.0
3	0.80	0.86	278.8	0.95	279.8	0.80	278.9
3	0.75	0.86	277.6	0.95	278.5	0.80	277.8

Table 6. **BRIGHTNESS DIFFERENCES FOR A 2-KM CLOUD TOP.** Differences were calculated with the results from Table 5.

	STANDARD		DRY		MOIST	
ε_3	$T_3 - T_5$	$T_3 - T_4$	$T_3 - T_5$	$T_3 - T_4$	$T_3 - T_5$	$T_3 - T_4$
0.90	−2.4	−3.1	−2.5	−2.6	−0.2	−1.7
0.85	−3.5	−4.1	−3.6	−3.7	−1.2	−2.7
0.80	−4.7	−5.3	−4.9	−5.0	−2.3	−3.8

under the same moisture profile as the clouds will be positive instead of close to zero (see Table 2). So, even if an individual FOV does not meet a $T_3 - T_4$ threshold for low clouds, its relationship with nearby clear FOVs clearly gives a contrast that aids in determining the presence of clouds (Lee, personal communication 1990).

If other conditions (moisture, droplet mode radius, optical thickness) remain constant, variations in cloud amount (scattered, broken, or overcast) will change the resulting brightness difference. The largest differences result from overcast and optically thick clouds with lesser differences for the broken and scattered cases. Clouds with the lower emissivity in channel 3 due to smaller droplet size, will produce larger differences as well. In formulating categories of cloud amount, thresholds will be determined depending on relative amount of moisture over optically thick clouds with a constant emissivity in channel 3 of .90. The radiative transfer results show that with an adjustment of about 1 to 1.5 K lower than thresholds set for a dry atmosphere, cloud amount will be more accurately determined in the more moist case.

In the results chapter, the effect of water vapor on brightness temperatures is incorporated into the low cloud analyses that follow.

IV. DATA AND METHODOLOGY

A. DATA CONSIDERATIONS

1. Satellite Data

The satellite data analyzed in this thesis depended on the type of weather phenomena predominant in any given pass. According to climatology, low clouds and fog dominate the northern oceans during the mid and late summer. The greater availability of data with more active weather systems rather than stable, low cloud areas and the preference for summer oceanic cases restricted the ease of obtaining the appropriate passes. However, selected satellite passes were found from the archive data of the First ISCCP (International Satellite Cloud Climatological Project) Regional Experiment (FIRE) and an archive from the western location of the Naval Oceanographic and Atmosphere Research Laboratory (NOARL West).

The FIRE data was stored in standard AVHRR High Resolution Picture Transmission (HRPT) format. The data was collected from the NOAA10 polar orbiter satellite which provided channels 3 and 4 but excluded channel 5. Unfortunately, the channel 3 sensor on NOAA10 was particularly noisy during this period. This experiment was focused on low clouds off the west coast of North America during the summer of 1987, so most of the passes contain widespread fog. Several scenes were selected from a FIRE pass which started at 0339 UTC or 2039 PDT on 18 July 1987. This time is particularly well suited for verification as visible satellite imagery was available earlier in the evening.

The data from NOARL was in Local Areal Coverage (LAC) format from the AVHRR on the NOAA11 polar orbiter, which contained all three IR channels and much less noisy channel 3 data. Passes covered the east coast of North America and western Atlantic from just north of Cuba to Greenland. The first detailed case comes from a pass which started at 0646 UTC or 0346 ADT on 29 June 89. Other scenes from passes over the western North Atlantic dated 18, 20 and 29 June 1989 between 0630 UTC and 0710 UTC were studied.

2. Verification Data

Generally, results showing negative brightness differences for the satellite channels could hardly be accounted for other than by the presence of low clouds or aerosols in any given scene over the ocean. However, to provide confidence in the analysis, other data was gathered to verify the actual presence of the low clouds. Normally, this is rather difficult due to the scarcity of surface and upper air observations in the oceans and the non-existence of visible imagery at night from NOAA satellites.

Visible Geostationary Observational Earth Satellite (GOES) imagery was primarily used to verify cloud conditions within scenes from the FIRE data, since the time of the pass was close to daylight hours. The visible imagery was compared to the scenes for easily recognizable cloud features and clear regions. With the North Atlantic Ocean cases, more buoy and ship reports were available by the nature of heavily travelled shipping lanes. In all cases, surface observations and upper air soundings over land near the coast were used as well. In all observations, and cloud and visibility observations were compared to the satellite analysis results.

B. METHODOLOGY

1. Choosing Scenes

Various subscenes were selected from overviews of satellite passes on the Interactive Digital Environmental Analysis (IDEA) Lab minicomputers at the Naval Postgraduate School using AVIAN software (Motell et al., 1991). The following criteria guided the choice of the cases:

- Areas with predominantly high clouds were avoided to focus on the low cloud-clear problem.
- Northern subscenes were favored to minimize the attenuation due to water vapor especially in channel 5. But in the case of the FIRE data, colder regions enhanced channel 3 noise.
- Areas where cloud tops temperatures were close to that of the ocean surface were chosen to test the improvements in low cloud analysis by by multiple versus a single IR channel. Over areas of warmer ocean surface temperatures, distinctly colder, low clouds would easily be discernible using single IR channel analysis.

- Coastal areas were preferred for easy reference to landmarks and observations in more data rich regions over land and sea.
- Due to high channel 3 solar reflectance, low clouds were not analyzed in daylight regions.
- Analysis times close to sunrise or sunset were desired for area comparisons with visible imagery.

2. Processing Subscenes

To test the utility of IR channel differences, multi-channel IR thresholds were used to improve upon the single channel analysis of thermal IR imagery for the low cloud analysis cases. For all cases, clear areas, low, middle, and high clouds were analyzed on channel 4 imagery and displayed. For the multi-channel analysis, middle and high clouds were retained as analyzed by T_4, but differences in channels 3 and 4 were used to improve the low cloud analysis. Based on the magnitude of this difference, categories of low cloud amount were designated.

The categories for the conventional analysis of channel four subscenes used key temperature thresholds. Brightness temperatures warmer than the SST minus 3 K initially specified the clear regions. The upper threshold for low clouds was set at approximately 800 mb temperature based on nearby soundings. Color enhancements were used to display these categories. Clear regions are depicted in blue, low clouds in red, and mid and high clouds in green. All clouds were displayed as a continuum of brightness temperatures in their respective categories to maximize cloud information. These thresholds are summarized in Table 7.

For the multi-channel data, the low cloud and clear categories were modified based on the brightness difference, $T_3 - T_4$, but the previous analysis of middle and high clouds was unchanged. Because moisture plays a role in the brightness difference, adjustments to the categories were made depending on the extent of atmospheric moisture above the clouds based on nearby soundings and water vapor imagery. Here, two sets of threshold categories were defined. Based on the radiative transfer experiments results of Chapter III, four categories were defined Table 7; clear, scattered clouds, broken clouds, and overcast. For the drier atmosphere, clear was defined by differences from +1.5 K (to account for boundary layer moisture over the ocean) to about -1 K, scattered clouds -1 K to

Table 7. THRESHOLDS FOR THE SINGLE AND MULTI-CHANNEL ANALYSES.

Single Channel Thresholds		
Category	T_4 (K)	
CLEAR	WARMER THAN SST-3	
LOW	SST-3 TO T_{800}	
HIGH	COOLER THAN T_{800}	
Multi-Channel Thresholds		
Category	$T_3 - T_4$ (K)	
	DRY	MOIST
CLEAR	+1.5 TO −1	+2 TO ±0
SCT	−1 TO −3	±0 TO −1.5
BKN	−3 TO −4.5	−1.5 TO −3
OVC	LESS THAN −4.5	LESS THAN −3

-3 K, broken -3 K to -4.5 K, and overcast less than -4.5 K. Characteristics of a moist atmosphere above the low clouds are dewpoint depressions of approximately 3 K throughout a reasonably thick layer. Thresholds for the moist case were, clear, differences from +2 K to 0 K, scattered clouds 0 K to -1.5 K, broken -1.5 K to -3 K, and overcast less than -3 K. It is possible that dry and moist regions exist in the same subscene in which case the appropriate scheme is applied depending on where the region of interest within the subscene lies. Color enhancements were used to make these categories easily distinguishable.

V. RESULTS

A. INITIAL CASES

The multi-channel IR data was applied to ten cases to evaluate its use for low cloud analysis. Two cases, one off the east coast and one off the west coast, are now presented in detail. Case 1, centered over the Bay of Fundy, describes a region of the ocean that is difficult to correctly determine regions of low cloudiness with one IR channel even with a detailed color enhancements. Case 2 off the coast of California illustrates an area of colder surface temperatures where it is difficult to separate areas of low cloudiness from cold SSTs. GOES imagery from the afternoon prior to Case 2 was used for ground truth, and surface observations were available to confirm the results of Case 1. After the results of these initial cases, highlights of the other eight cases are discussed.

1. Case 1

The standard channel 4 IR view for Case 1 including surface observations for 0700 UTC is illustrated in Fig. 5a. Middle to high clouds, clearly denoted in the IR image, cover the southeast portion of the scene over the eastern part of Nova Scotia as well as off the coast of Maine and New Brunswick. However, one can only suspect low clouds over portions of the Bay of Fundy. Also, warmer temperature signatures, appearing as dark regions over the bay extend from St John, New Brunswick (YSJ) and from St Martin's further north up the coast.

Stations in the surrounding bay regions generally reported low ceilings and visibilities. YSJ on the north coast of the bay reported a 100 ft ceiling and near zero visibility in fog. In the northern portion of the Bay of Fundy, Moncton, New Brunswick, (YQM) reported a broken ceiling at 300 ft. At the tip of the peninsula of Nova Scotia, Yarmouth (YQI) reported 6 m in fog but no ceiling. A station on Prince Edward Island reported a scattered deck at 300 ft and visibility of 3 m in fog. Ship reports south of Nova Scotia reported visibilities of about a mile. Other stations inland to the west and over water in the southwest reported no ceilings and no obstructions to visibility.

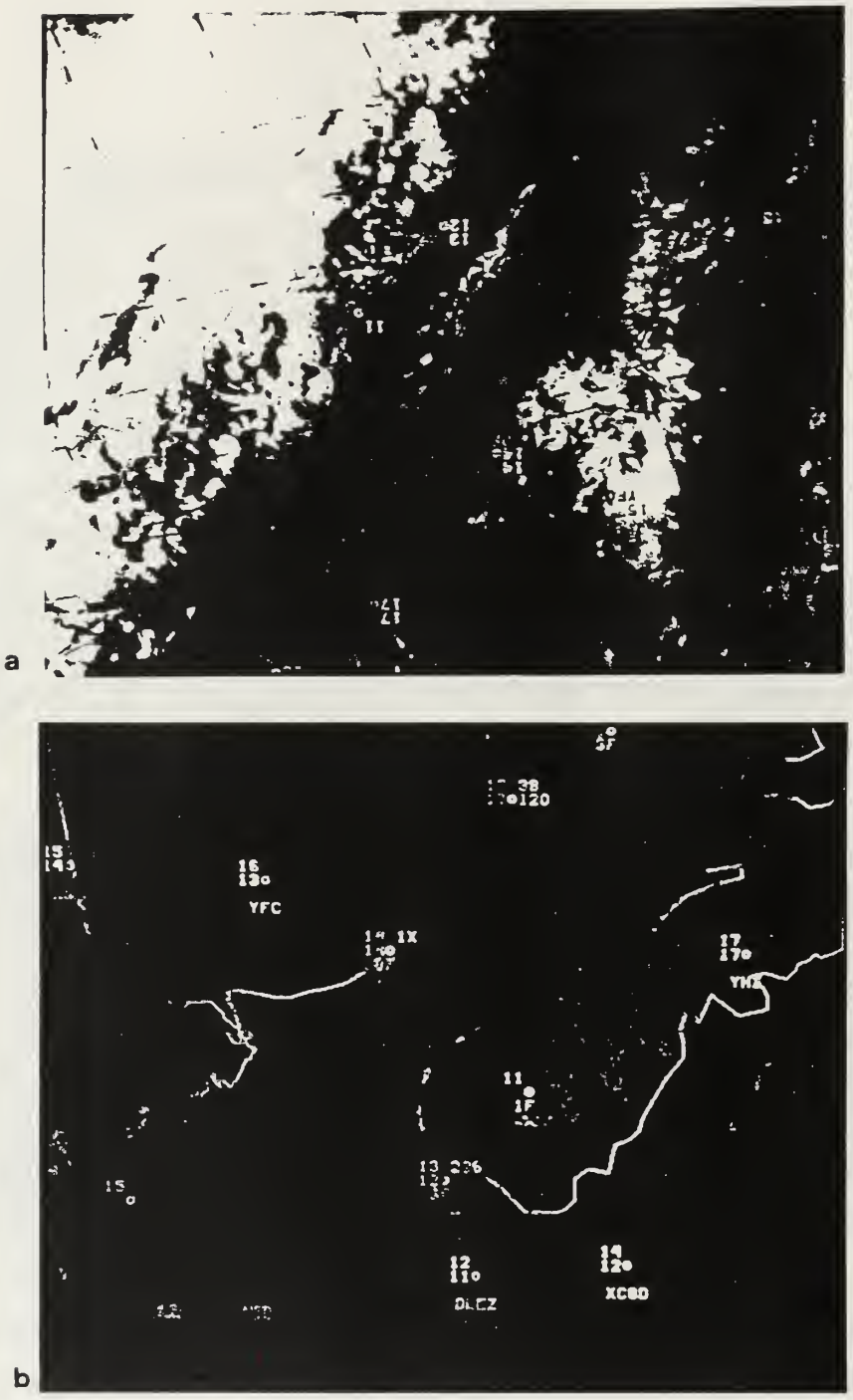

Fig. 5. Case 1 single channel analysis, Bay of Fundy. a: Single IR channel 4 image, and b: Color enhancement applying the thresholds from Table 7.

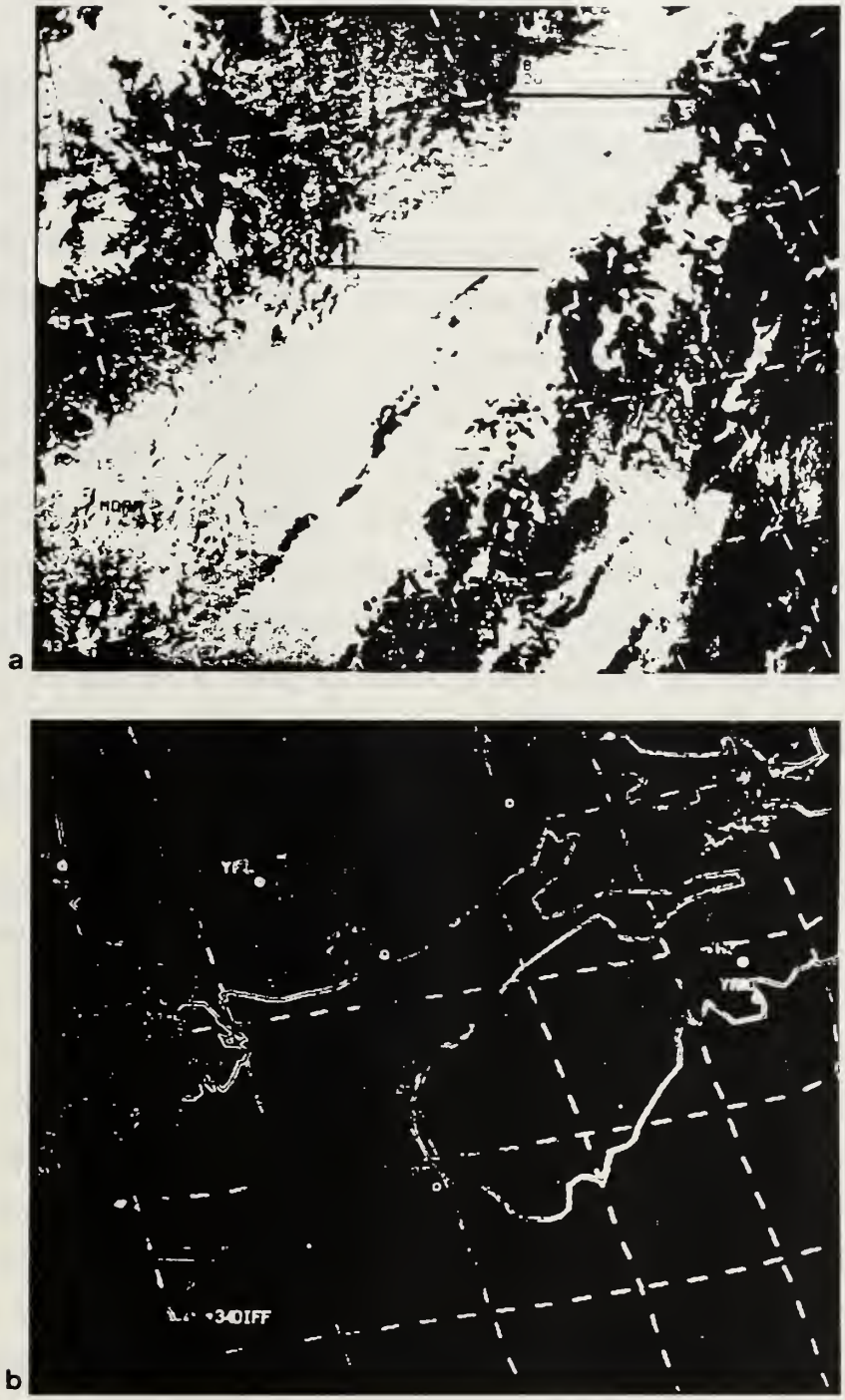

Fig. 6. Case 1 multi-channel analysis, Bay of Fundy. a: Channel 3-4 temperature difference image, and b: Color enhancement applying the thresholds from Table 7 for the dry case. The middle and high cloud enhancement was retained from the single channel analysis.

First, a cloud analysis was prepared using one IR channel as a standard to evaluate the multi-channel analysis. A representative SST was chosen for the (SST-3 K) clear-low cloud threshold. Since there is a variation of SST over the scene as well as warm low cloud tops, this threshold represents the best possible analysis with one channel. This is shown in Fig. 5b. The 800 mb temperature from the Portland, Maine (PWM) sounding at 12 UTC (Fig. 7a) was used as a guide in determining an upper low cloud threshold. Temperatures greater than 284.5 K are indicated by blue and specify the clear areas, which borders what appears to be SST variations. Low cloud top temperatures are specified by shades of red with temperatures ranging from 284.5 K to 278.7 K. Clouds were analyzed in the lower half of the bay, around the peninsula and along the coast of Maine. Middle and high clouds are in shades of green according their cloud top temperatures colder than 278.7 K.

The $T_3 - T_4$ image (Fig. 6a.) gives a different perspective of this case. White pixels denote areas where $T_3 < T_4$, i. e. differences are negative. Widespread areas of negative differences depict the low clouds, which are evident over the entire Bay of Fundy and northward over the isthmus to Prince Edward Island. Within the low cloud deck are apparent plumes coming from YSJ and St Martin's up the coast. Additional low cloud regions, not at all evident in the previous analysis, extend from the bay inland over the peninsula of Nova Scotia and southwestward to YQI. Middle clouds are solid white consistent with our radiative transfer results that higher cloud tops will show more negative differences. Positive differences are denoted by the darkened pixels. Note the significant area of positive difference to the west of YSJ and over the eastern side of the scene. High thin clouds and atmospheric moisture attenuating upwelling radiation in channel 4 cause the larger positive differences as $T_3 < T_4$. Other studies (e. g. Wieman 1990 and others) have used the positive differences to improve analyses of thin cirrus clouds.

To further illustrate the details of the channel 3-4 differences, profiles of brightness temperature were taken along lines indicated in Fig. 6a for both channels 3 and 4. Graphs of the profiles are displayed in Fig. 8. Through Line

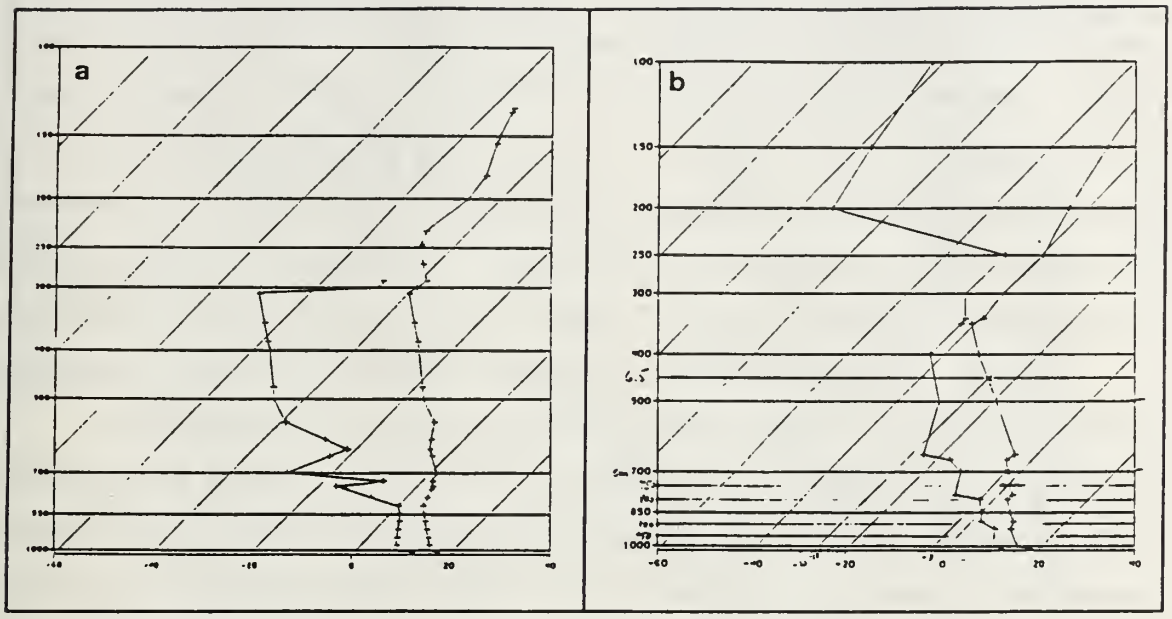

Fig. 7. Soundings used in Cases 1 and 2. a: Portland, Maine, 12 UTC 29 June 89, and b: Oakland, California, 00 UTC 18 July 87.

A over the isthmus, the northern most line, the difference is as large as -4 K. At the western most portion of line A, differences are nearly zero indicating no low cloudiness. Going eastward satellite channel temperatures drop for both channels and then increase again, but the differences remain large revealing an area of overcast clouds. YQM reported 300 broken with 1200 overcast just on the western edge of the low cloud region. The western most portion of Line B protrudes in middle and high thin clouds which explains the positive differences and the somewhat colder temperatures. Further east on line B just south of YSJ on the northern coast of Nova Scotia, differences are as large as -5 K with a small clear zone indicated by zero differences.

The complete multi-channel analysis is illustrated in Fig. 6b. The brightness difference thresholds for clouds from Table 7under a relatively dry atmosphere were used the analysis. Middle and high clouds are the enhanced portions of the standard IR imagery and follow from Fig. 5b. The multi-channel analysis successfully analyzes a variety of low cloud detail for this case. Low clouds are the thickest or the most overcast further inland into the Bay of Fundy.

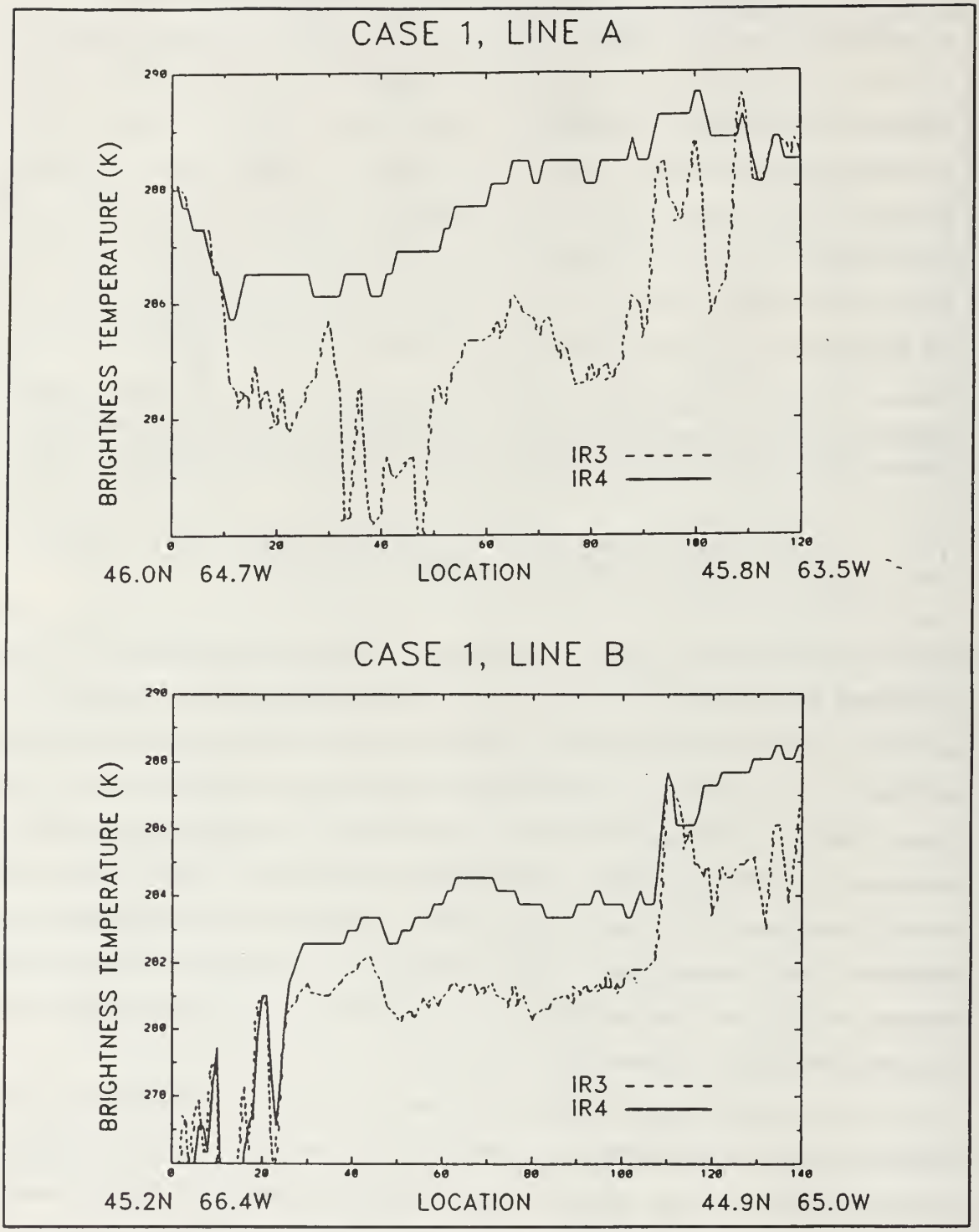

Fig. 8. Profiles of brightness temperatures along lines for Case 1.

Coming off YJS and St Martin's, plumes are identified as overcast amongst the broken surrounding low clouds, possibly because these plumes may exhibit properties of aerosols with lower emissivities than the low clouds. The clear regions (in black) are easily identified over land and south over the ocean; channel differences in these regions greater than -1 K. Bordering the middle and high clouds are gray pixels not categorized. These FOVs did not show up cold enough to be identified as a middle or high cloud. However, $T_3 - T_4$ is too positive to be anything else. They occur within thin high cloud areas of this case.

Cloud features over land and ocean in this case were well analyzed by the multi-channel analysis. SSTs labeled clouds and clouds labeled clear using the channel 4 enhancement were improved in the channel 3-4 difference analysis with overall good agreement with surface observations. All deficiencies in the single channel analysis were corrected by the multi-channel analysis. In addition thick plumes and clear regions within the low cloud area were identified.

2. Case 2

This subscene includes a portion of the eastern Pacific Ocean off the coast of California around San Francisco. The standard channel 4 view of the image is illustrated in Fig. 9a. Cloud features depicted include areas of stratus and stratocumulus protruding southward just off the coast of northern California. Low, middle, and high clouds cover the northern most portion of the state. Reporting stations in Eureka (APC) and Ukiah (UKI) are located just inland of the coast in less cloudy areas reporting higher scattered clouds. Near the northern coast, there appears colder upwelling waters typical for summer off that coast.

The standard IR image was color enhanced in much the same way as in Case 1 (Fig. 9b). Brightness temperatures warmer than 281.4 K were classified in blue as clear. The low-middle cloud threshold of 275.1 K was determined from the Oakland (OAK) sounding shown in Fig. 7b. Low cloud areas are depicted in red. Colder than 275.1 K, middle and high level clouds were analyzed in green. Note that for this northern California case, atmospheric temperatures in this case were colder than in Case 1.

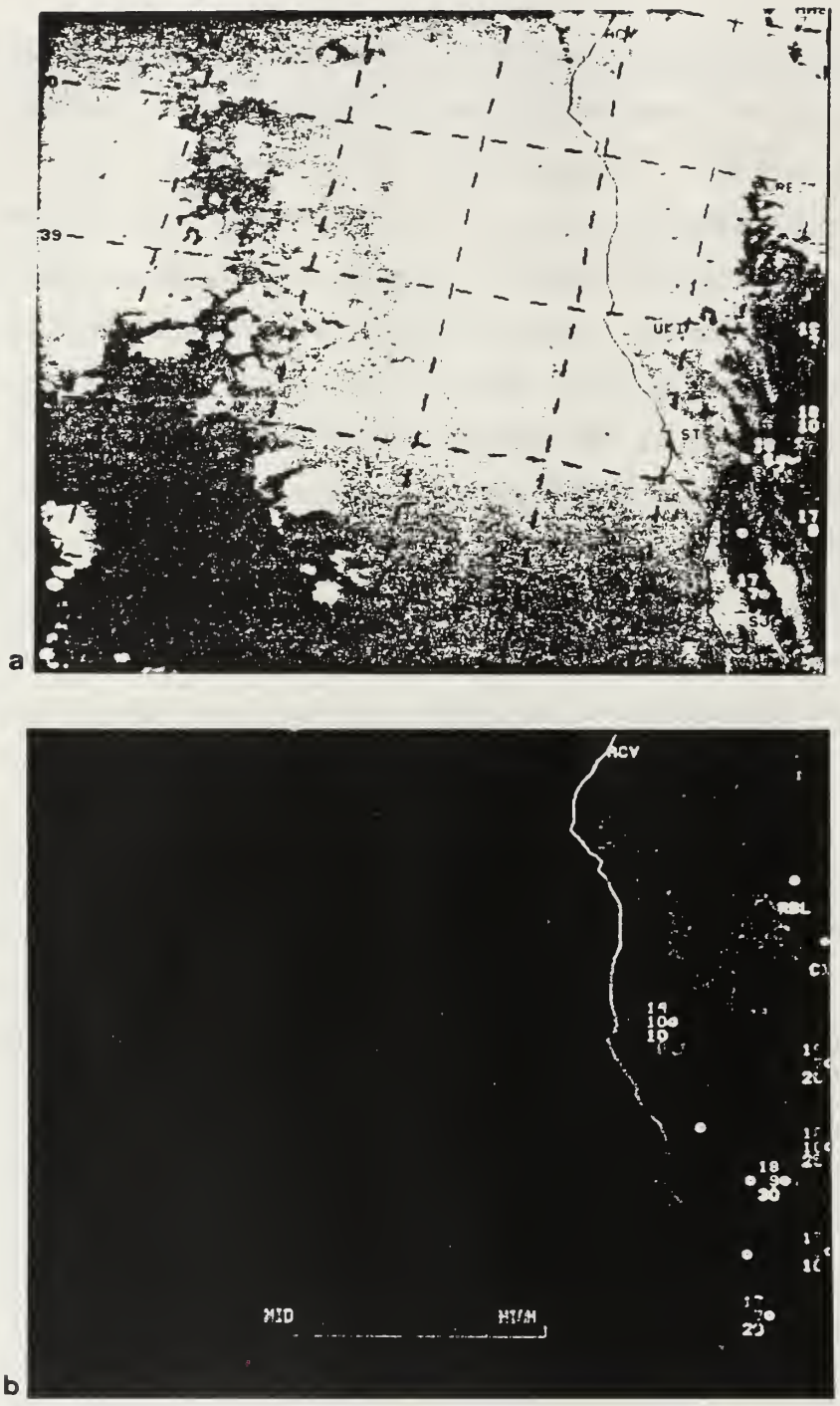

Fig. 9. Case 2 Single Channel Analysis, coast of northern California. a: Single IR Channel 4 Image. b: Color Enhancement Applying the Thresholds from Table 7.

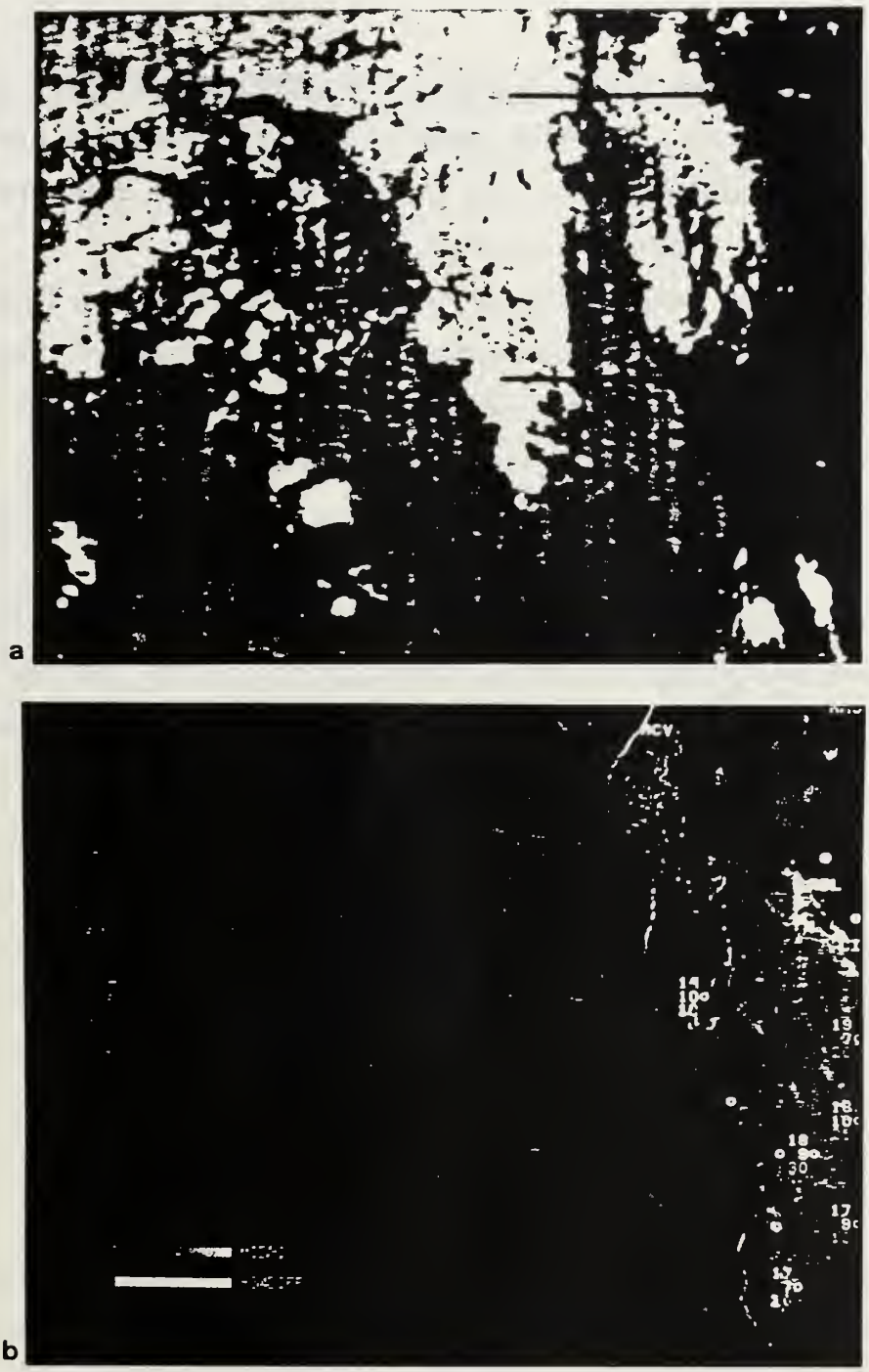

Fig. 10. Case 2 Multi-Channel Analysis, coast of northern California. A: Channel 3-4 Temperature Difference Image. B: Color Enhancement Applying the Thresholds from Table 7 for the moist case. The middle and high cloud enhancement was retained from the single channel analysis.

The single channel analysis is unclear about the locations of low clouds and clear areas. Near the coast, what appeared as a SST signature is analyzed as low cloud. Low cloud analysis on the seaward, western part of the image is reasonably successful. High clouds are easily identified.

The differenced image, shown in Fig. 10a, aids in confirming what was cloud and clear despite the noise present due to channel 3. Suspected clouds off the coast were confirmed to be non-existent. Clouds that were already easily identified are enhanced. The positive difference regions in darker gray shade levels delineate high clouds over northern California and clear regions over central California.

Profiles of brightness temperature for both channels 3 and 4 were taken along lines as drawn on the channel 3-4 difference image in Fig. 10 over areas of low clouds. Graphs of the profiles are displayed in Fig. 11. At the western portion of line A over the low clouds, the brightness difference is no more than -3 K. Differences are slightly negative over the clear ocean becoming slightly positive at clear land. More low clouds inland give negative differences to -4.5 K. At the eastern portion of this profile, large positive differences are caused by high thin clouds. On the eastern half of the profile of line B, differences are slightly negative, which was a common occurrence over clear oceans in many of the cases in this thesis. Scattered low clouds are indicated by the negative differences in the western half of line B, but the two positive spikes cannot be explained except by noise.

The color enhancement for this case is presented by Fig. 6b. The enhancement allows improved analysis of low clouds for the case. Since moisture was measured over the region by the OAK sounding, the thresholds for a moist atmosphere were used. Due to channel 3 noise, the scattered category was eliminated. The area of low SSTs is now analyzed as being clear. The location of the most overcast low clouds now become evident at a glance, such as along the eastern portion of the extension of low clouds just off the northern California coast. A clear slot extending northward along the coast is another feature which

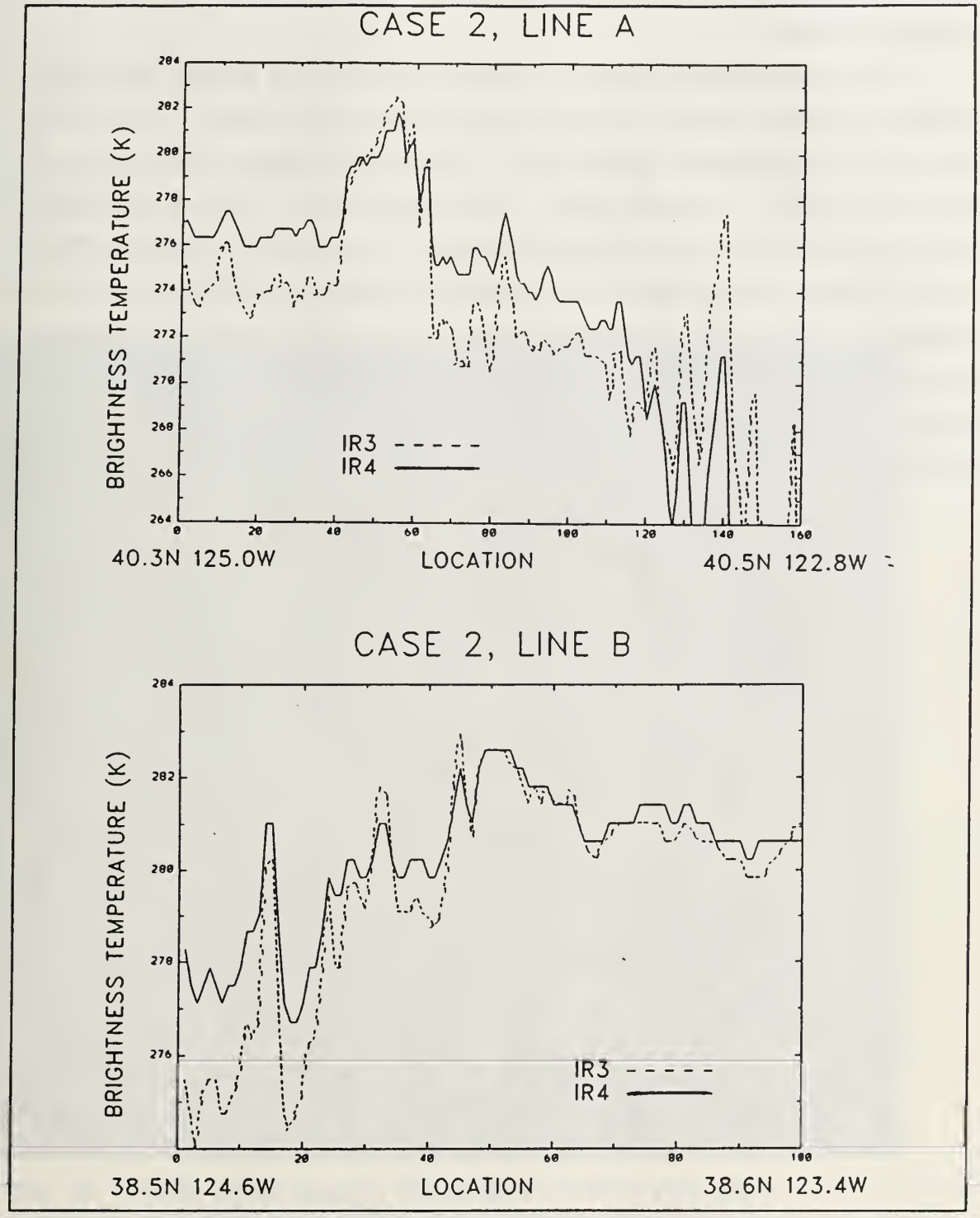

Fig. 11. Profiles of brightness temperatures along lines for Case 2.

is poorly analyzed with the single IR channel but clearly depicted by the multi-channel approach.

The multi-channel analysis results are supported by ground truth observations and GOES imagery from three hours earlier that evening at 0045 UTC. From the GOES imagery shown in Fig. 12, no cloud features existed in the region of cold SSTs. The clear region up the coast analyzed by the multi-channel analysis was also defined by the GOES image. The area of low cloudiness off the coast retained its general form till the time of the subscene and one can match the larger cloud areas. The few observations on the coast supported analysis that showed the lack of clouds there. Overall, there was strong agreement between the multi-channel analysis and the GOES visible imagery and fair agreement with surface observations.

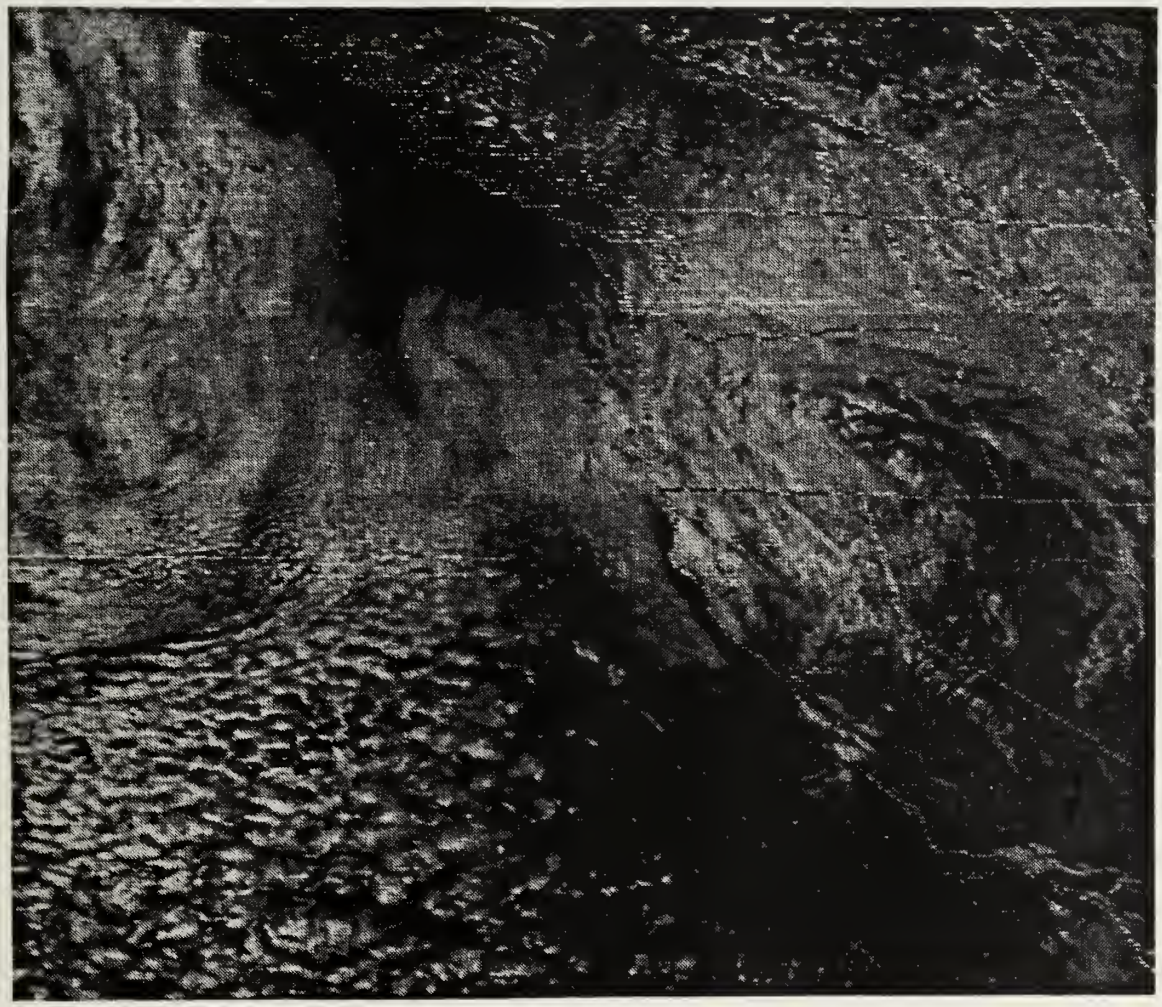

Fig. 12. Visible GOES imagery. Dated 0045 UTC 18 July 1987.

B. SUMMARY OF ALL CASES

Results of all the cases studied in this thesis are summarized in Table 8. Each case is described by date and the latitude and longitude of the upper right corner of the subscene rounded to the nearest degree. For each case an evaluation is made for the single channel enhancement and the multi-channel improved enhancement.

For the channel 4 enhancement, common problems such as SSTs labeled as cloud and clouds labeled as clear are noted. The decision is based on the concurrent surface observations, general consensus of the scene and comparison to the enhanced channel 3-4 difference.

For the two cases from the FIRE data, a determination was made on how the multi-channel analysis agreed with GOES visual imagery from several hours before FIRE cases. Comparison results with GOES imagery could only be subjective since it was three hours different from that of the subscenes and the images were in a different satellite projection. A "strong" agreement to GOES visual meant that cloud features and clear regions compared essentially the same as far as the observer could see. A "moderate" agreement indicated some discrepancies between the multi-channel IR and the GOES visual as is described for Case 6.

The east coast cases used surface observations to confirm the multi-channel analyses. Variable number observations were available depending on the scene location and time; therefore, objectivity was difficult. "Excellent" agreement says that all the observations were consistent with the difference enhancement, while "good" describes 70% agreement. The "fair" category indicates better than 50% agreement but also allowed for instances when observations were too scarce or not collocated to be relevant.

The category, "Improvement on Chan 4" describes the degree to which deficiencies were eliminated using the multi-channel analysis. Areas where the channel 4 only images were clearly in error i. e. clouds labeled as clear or SST labeled as cloud, were studied with the multiple channel enhancement. In four cases, the improvement was large and all the problem areas were corrected. Five additional cases showed noticeable improvement but some deficiencies remained.

Table 8. SUMMARY OF RESULTS.

Case no.	Date	Lat/Lon (upper right)	Chan 4 Enhancement		Chan 3-4 Diff Enhancement		
			S. S. T. Labeled Cloud	Cloud Labeled Clear	GOES Vis Agree-ment	Obs Agree-ment	Improve-ment on Chan 4
1	29JUN89	48N/67W	YES	YES	NA	GOOD	ALL
2	18JUL87	37N/121W	YES	POS	STRONG	FAIR	MOST
3	18JUN89	46N/65W	POS	YES	NA	EXCEL	ALL
4	18JUN89	49N/62W	YES	YES	NA	EXCEL	MOST
5	18JUN89	51N/65W	YES	YES	NA	GOOD	ALL
6	18JUL87	47N/124W	YES	YES	MOD	FAIR	SOME
7	20JUN89	49N/61W	NO	YES	NA	GOOD	MOST
8	18JUN89	43N/65W	YES	YES	NA	EXCEL	ALL
9	20JUN89	44N/64W	YES	YES	NA	POOR	MOST
10	30JUN89	53N/55W	YES	YES	NA	FAIR	MOST

One case only exhibited modest or "some" improvement. In every case there always some improvement.

Cloud features were well analyzed by the channel 3-4 difference in Cases 3 through 5, such that most or all the deficiencies in the single channel enhancement were improved bringing out hidden cloud features. Using the single channel approach, large regions appeared clear and it was difficult to decide where to set the threshold between clear and cloudy. These scenes were chosen from regions north of the Gulf Stream which in itself gives the appearance of a distinct low cloud boundary. Case 4 included ship tracks, contrails, and a band of thick clouds which appeared warm in channel 4 in comparison to nearby cloud regions.

For these cases one discrepancy remains. Bordering contrails and high cloudiness are pixels of positive differences that were not enhanced, because these pixels were too warm for the high cloud threshold in the single channel analysis but now are too positive to fit into the clear category. These positive differences are attributed to either very high moisture or very thin clouds. The cirrus effect was investigated by Wieman (1990) who used the attenuation of channel 4 and 5 radiances by cirrus ice crystals for the analysis of high clouds. This so-called discrepancy actually adds more information to the analysis.

Channel 3 noise was a major factor in Case 6, the other FIRE case. But, an additional problem was noted as well. The SST signature thought to be cloud bordering Vancouver Island is now confirmed cloudless. However, half of this subscene was strongly affected by upper level moisture and was difficult to classify. Also, positive differences were not consistent over clear land. This may require applying different sets of threshold categories depending on the area of interest.

The rest of the cases gave a very positive rendition of low clouds. Cases 7, 9, and 10 had lower observation agreement results, but low cloud areas are generally close to frontal systems where low clouds are reasonably expected. The single channel analysis in case 8 analyzes a developing cold core ring, a strong Gulf Stream SST anomaly, cold enough to be analyzed as low clouds by the single channel analysis. Interestingly, the multi-channel enhancement indicated scattered low clouds following the SST signature. This may have cast doubt on the viability of the scattered category if it weren't for a well-placed observations confirming low visibilities and scattered clouds.

VI. CONCLUSIONS AND RECOMMENDATIONS

Multi-channel imagery was used to analyze nighttime low clouds whose cloud top temperatures were near to or greater than that of the ocean surface. A threshold scheme delineated low cloud amount assuming other cloud properties remained fairly constant. This led to an improvement to the single channel IR analysis. Low cloud extent categories were broken down to scattered, broken, and overcast depending on the brightness difference. This breakdown is a reflection of partially filled FOVs but does not account for the possibility of optically thin clouds and relatively higher low clouds. Moisture attenuation, cloud properties and other factors complicate the enhancement scheme. The moisture attenuation problem was addressed directly with LOWTRAN7 model simulations of different atmospheric moisture profiles. Two different sets of thresholds from the radiative transfer results were developed for the "dry" and "moist" cases, results. The overall temperature difference enhancement scheme combined with the single IR channel mid and high cloud enhancements gave a successful analysis of low cloud areas. But other issues still remain.

Suggested future work should concentrate on better accounting for the effects of moisture. In this thesis, only "dry" and "moist" conditions were considered in a choice of thresholds. More realistic radiative transfer simulations should be run to quantify changes in attenuation from a real time sounding. Also, more variations in moisture confined to the boundary layer of the model profile would be useful. But, because there can be such a wide variation in moisture profiles in any given scene, a pixel by pixel account of integrated moisture is needed to effectively correct the moisture attenuating effect on the brightness difference. This data may be derived from a satellite water vapor channel and other sources. Better yet, atmospheric moisture amounts can be derived through the channel 4-5 difference. This difference would provide a measure of moisture attenuation for the entire image, and aid in adjusting the channel 3-4 difference for moisture for

every pixel in the image. Thin cirrus has a similar effect as moisture (Wieman 1990) and could automatically be included into the adjustment as well.

Higher stratus clouds show more negative differences since there is less integrated attenuation effects in channel 4 or 5, such as moisture. D'Entremont (1986) devised a technique to analyze cloud top heights and cloud amounts together. His technique in conjunction with adjustments for moisture may help fine tune the analysis of most low clouds.

Optical depth of clouds or fog depends on geometric cloud thickness, droplet density, and droplet mode radius. It was assumed that droplet size and density were not variables and that clouds were usually optically thick when the threshold categories were constructed. However, changes in optical depth may introduce a significant error in the brightness differences. To better quantify the effect of optical depth on the threshold categories, field measurements, such as were taken during the FIRE experiment, need to be made to compare actual cloud properties to satellite measured radiances from scenes within the same region.

In the many cases, brightness differences of clear pixels were slightly negative over ocean and at the same time positive over land. Aerosols reside close near the surface, especially over ocean. This aerosol field, handled by LOWTRAN7's Navy Maritime Model, may have an optical depth large enough to lower transmittance significantly in channel 3 so that the upwelling radiance may be more attenuated than in channels 4. Model simulations are needed to investigate this possibility.

The multispectral analysis technique was quite successful for most of the cases in this thesis. More sophisticated satellite multi-channel analyses, as outlined above, offers promise to improve these analyses further. These objective cloud analyses can substantially enhance operational meteorological support.

REFERENCES

Allam, R. J., 1986: On the slight misregistration of AVHRR channels 3 and 4. *Int. Journ. Remote Sensing*, **7**, 887-894.

Crosiar, C., T. F. Lee, and A. Caughey, 1989: Nighttime cloud classification using two infrared channels of the AVHRR. *Twelfth Meteorological Conference in Weather Analysis and Forecasting*, Preprint Vol., 330-333.

D'Entremont, Robert P., 1986: Low- and midlevel cloud analysis using nighttime multispectral imagery. *Journ. Climate and Applied Met.*, **25**, 1853-1869.

_____, and L. W. Thomason, 1987: Interpreting meteorological satellite images using a color-composite technique. *Bull. American Meteor. Soc.*, **68**, 762-768.

Dozier, J., 1981: A method for satellite identification of surface temperature fields of subpixel resolution. *Remote Sensing of Environ.*, **11**, 221-229.

Ellrod, G., E. Maturi and LT(jg) J. Steger, 1989: Detection of fog at night using dual channel GOES-VAS imagery. *Twelfth Meteorological Conference in Weather Analysis and Forecasting*, Preprint Vol., 515-520.

Eyre, J. R., J. L. Brownscombe and R. J. Allam, 1984: Detection of fog at night using advanced very high resolution radiometer imagery. *Meteorological Magazine*, **113**, 266-271.

Hunt, G. E., 1973: Radiative properties of terrestrial clouds at visible and infrared thermal window wavelengths. *Quart. Journ. Royal Meteor. Soc.*, **99**, 346-359.

Motell, C. E., D. Burks, P. A. Durkee, and C. H. Wash, 1991: AVHRR image navigation by satellite attitude correction. Part I: Manual landmarking. *Journ. Meteor. and Oceanic Technology*, submitted.

Olesen, F.-S. and H. Grassl, 1984: Cloud detection and classification over oceans at night with NOAA-7. *Int. Journ. Remote Sensing*, **6**, 1435-1444.

Saunders, R. W., and K. T. Kriebel, 1988: An improved method for detecting clear sky and cloudy radiances from AVHRR data. *Int. Journ. Remote Sensing*, **9**, 123-150.

Wieman, S., 1990: Multispectral analysis of thin cirrus. M.S. Thesis, Naval Postgraduate School, Monterey, CA, 50pp.

INITIAL DISTRIBUTION LIST

		No. Copies
1.	Defense Technical Information Center Cameron Station Alexandria, VA 22304-6145	2
2.	Library, Code 52 Naval Postgraduate School Monterey, CA 93943-5002	2
3.	Chairman (Code MR/Hy) Department of Meteorology Naval Postgraduate School Monterey. CA 93943-5000	1
4.	Professor Carlyle H. Wash (Code MR/Wx) Department of Meteorology Naval Postgraduate School Monterey, CA 93943-5000	1
5.	Professor Philip A. Durkee(Code MR/De) Department of Meteorology Naval Postgraduate School Monterey, CA 93943-5000	1
6.	Capt James D. Dykes, USAF 3350 Technical Training GP (ATC) Chanute Air Force Base, IL 61868	1
7.	Commanding Officer AFIT/CIR Wright-Patterson Air Force Base, OH 45433-6583	1
8.	Commander Air Weather Service Scott Air Force Base, IL 62225	1
9.	Commanding Officer Air Force Global Weather Central Offutt Air Force Base, NE 68113-5000	1

10. USAF ETAC/LD 1
Air Weather Service Technical Library
Scott Air Force Base, IL 62225

11. Mr Thomas Lee 1
Naval Oceanographic and Atmospheric
Research Laboratory
Atmoshperic Directorate
Monterey, CA 93943-5006

12. Mr Lee Eddington 1
Code 035
Naval Postgraduate School
Monterey, CA 93943

498-730